Mechanics of Advanced Composite Structures

Semnan University

journal homepage: http://MACS.journals.semnan.ac.ir

Investigation of Nonlinear Behavior of Composite Bracing Structures with Concrete Columns and Steel Beams (RCS) Applying Finite Element Method

A. Kheyroddin, M.A. Kafi, F. Eskandarian, Z. Madah*

Department of Civil Engineering, Semnan University, Semnan, Iran

KEYWORDS

Composite frame of RCS
Nonlinear analysis
Steel beam
Concrete column
Bracing
Finite element method

ABSTRACT

The composite structural system (RCS) is a new type of moment frame, which is a combination of concrete columns (RC) and steel beams (S). These structural systems have the advantages of both concrete and steel frames. In previous research on composite structures, there are some studies regarding RCS composite connections. In this paper, the seismic behavior of the RCS composite bracing frame is inspected. In order to carry it out, nonlinear analysis of RCS composite frames with and without bracing has been operated applying finite element method (FEM). Behavior factors of these frames have been computed after analyzing frames. It can be observed that braces increase the yielding strength, ultimate strength, and stiffness of RCS composite frames. moreover, the comparison of analytical and experimental results reveals that the nonlinear behavior of RCS can be accurately predicted applying finite element method (FEM).

1. Introduction

Composite structures, a combination of reinforced concrete and steel members, had been used increasingly over the past decade [1]. These two materials could be applied in different ways in order to generate different types of composite structures. The application of concrete column and the application of steel beam would cause the capacity of each of these materials properly (i.e., concrete in pressure and steel in tension) [2, 3].The use of concrete columns increased the stiffness and damping of the structure and reduced the cost of materials as well. Moreover, the presence of a steel beam increased the energy absorption of these types of frames. Applying the composite moment frame (RCS) had begun in the United States since the 1970s and 80s as an alternative for the steel frame in high-rise buildings and it had been applied in Japan instead of concrete frames in short buildings with 3,4 and 5 stories [4].

In order to conduct a study, various research methods could be applied regarding composite structures. Mokhtar Bouazza and his co-workers inspected on composite structures [5]. They presented an exact analytical solution for mechanical buckling analysis of symmetrically cross-ply laminated plates, including curvature effects. In other studies, They were also working on Analytical solution of refined hyperbolic shear deformation theory to acquire the critical buckling temperature of cross-ply laminated plates with simply supported edge [6]. These researchers have other studies, too [7-9].

Hemmati and Kheyroddin inspected on transition story effect on the behavior of composite tall building. They were working on linear and nonlinear behavior of 5, 10 and 15-story buildings that have RC frames with shear walls in lower stories and steel frames with bracings in upper stories. Analytical results revealed that applying transition story between two different parts of hybrid structures ameliorated the seismic behavior of these buildings [10]. Bakhshayesh and Mirghaderi examined on Experimental investigation of steel beam to RC column connection via a through-plate. In the current paper, two interior connections at a 3/4 scale were evaluated experimentally under cyclic lateral loading and a constant axial load on the column. In the specimens, the beams were connected to a vertical plate passing through the concrete column (Through Plate).

* Corresponding author. Tel.: +98-863-2625720; Fax: +98-86-34173450
E-mail address: zeinab1365_madah@yahoo.com

DOI: 10.22075/MACS.2019.17137.1197
Received 2019-02-04; Received in revised form 2019-06-28; Accepted 2019-07-28

The portions of mentioned mechanisms of the entire connection moment were 65%, 20%, and 15%, respectively. By proportioning the connection components based on the presented design procedure, plastic hinges were created in the beams, and the connection components remained undamaged. The through plate involved with concrete provided a strong panel zone with elastic behavior, and the suggested connection was categorized as a fully restrained connection. The tested specimens provided permanent hysteretic diagrams without any pinching [11].

Cheng and Chen inspected the Seismic behavior of steel beam and reinforced concrete column connections. In a general look, six cruciform RCS joint sub-assemblages were constructed and tested. Parameters considered included composite effects of the slab and beam, the tie configuration in the panel zone, effects of the cross-beam, and the loading protocol. Test results indicated that all specimens performed in a ductile manner with plastic hinges formed in the beam end near the column face. It was found that the ultimate strength of the composite beam was enhanced by 27% on average, compared with that of the steel beam without the slab [12].

Bazzaz and his co-workers studied on Evaluating the performance of OBS-C-O in steel frames under monotonic load. some numerical studies had been performed applying ANSYS software, a frame with off-center bracing system and optimum eccentricity (OBS-C-O), and another frame with the same identifications without ductile element (OBS) had been generated. the analytical results revealed that the performance of steel ring at the end of off-center braces system was illustrating as a first defensive line and buckling fuse in the off-center bracing system [13]. Ghods and her co-workers studied Nonlinear behavior of connections in RCS frames with bracing and steel plate shear wall. Pursuant to verified finite element model a parametric study had been carried out on five RCS frames with different types of lateral restraint systems. The main objective of this study was to investigate the forming of plastic hinges, distribution of stresses, ductility, and stiffness of these models [14]. Nguyen Studied on a paper with title of Numerical Study on a New Through-Column-Type Joint for RCS Frame. The investigated beam–column joint detail was a through-column type in which an H steel profile totally embedded inside RC column was directly welded to the steel beam. The H steel profile was covered by two supplementary plates in the joint area. This detail provides two main advantages: The column was continuous, and no stirrups in the joint area were needed [15]. Mirghaderi and his co- workers analyzed a Moment-connection between continuous steel beams and reinforced concrete columns under cyclic loading. They suggested a new moment connection between steel beams and a reinforced concrete column (RCS). In this proposed connection, two parallel beams passed from both sides of the column and were welded to the cover plates surrounding the concrete column in the joint area [16]. There are a lot of done studies regarding composite structures, as well[17].

By deliberating this issue that Iran's regulations of composite structures do not provide comprehensive information for Iranian structural engineers. In this research, the attempt was to provide information about structural behavior and ductility by FEM analysis of RCS structures. Moreover, in the context of reinforcing the existing weak RCS structures, bracing could be defined as a solution.

2. Model Verification

One of the essential issues in modeling and analyzing is the calibration (verification) of the studied model. This category is significant due to the possibility that the accuracy of applied software is not safe and acceptable; the obtained analytical results cannot be reliable. In order to verification of the analytical model, an experimental specimen (a common study of the United States and japan) had been examined on the $\frac{1}{3}$-scale frame with steel beams and concrete columns (Fig. 1). This experiment had been tested by Iizuka and his colleagues at the Institute of Technical Research and Development “Nishimatsu” [18]. This specimen was modeled and analyzed in the software ABAQUS. The finite element meshing of this specimen was displayed in Fig. 1. They tested two frames with 2 stories and 2 spans, with different details of connections, including "through beam type" and "through column type".

It was chosen the through column connection for analysis of RCS frames. Since joints of steel beam and concrete column connected together by welding face bearing plate at the steel beam flange in the frame structure, beam–column and face bearing plate had a good confined with joint regions to make joint regions little slip. The details of the connection between the steel beam and reinforced concrete columns are shown in Fig. 2. It is indicated that concrete and steel in the joint regions could still work together until the destruction of the beam–column joint.

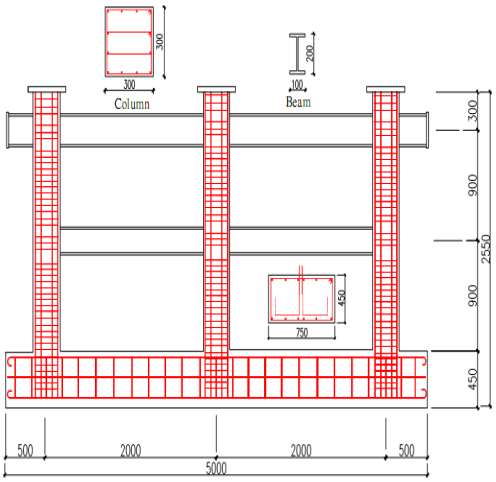

Fig. 1. 2-story frame with 2-span and its details of connections in the Nishimatsu Institute of Technical Research [19].

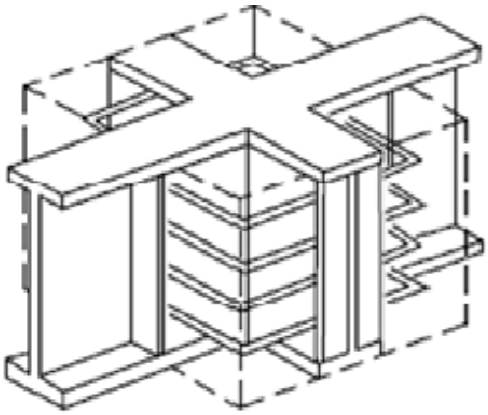

Fig. 2. The connection details of column and beam[19]

The failure mode was based on a plastic hinge formed at the end of the beam. However, in the latter, failure mode was shear failure, and plastic hinges formed at the end of the column. This shear failure consists of steel covering plate and steel belts. In addition, it was found that the hysteresis diagram of the connection with the through column consisted of larger area than connection with the through beam (Fig. 3). Consequently, the connection with the through column had better seismic performance than connection with the through beam [19].

3. Modelling Numerical Elements

For concrete columns and steel beams, three-dimensional non-linear elements and 8-node homogeneous elements (C3D8R) were applied. Linear elements and truss elements with double nodes were used for longitudinal and transverse reinforcements. For modeling and verification of composite experimental frames (RCS), the main members of this structure were modeled in ABAQUS including; concrete columns, contact plates between concrete and steel in the panel zone, steel beams, supporting sheets and longitudinal and transverse reinforcements (Fig. 4) [20].

3.1. The material of reinforcement and structural steel

In conventional concrete models, the behavior under compressive stresses was usually represented by the plasticity model, while the behavior under tensile stresses was expressed by the smeared cracking model. The smeared cracking model, however, encountered numerical difficulties on the analysis under cyclic load.

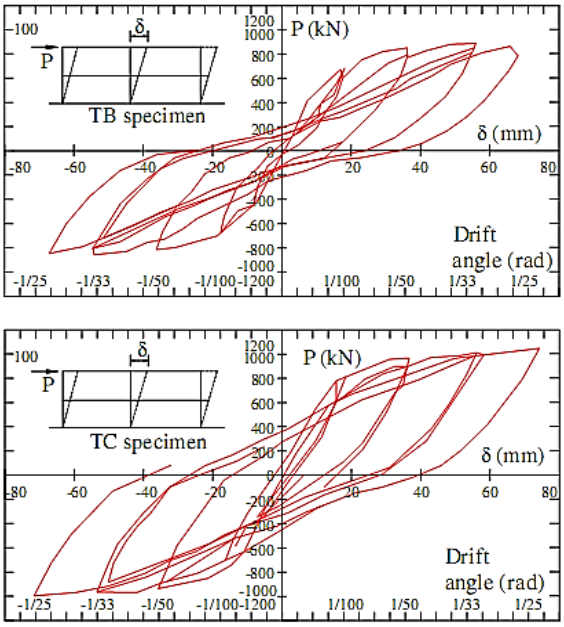

Fig. 3. Hysteresis curves for 2 connections under cyclic load in the Nishimatsu Institute of Technical Research[19].

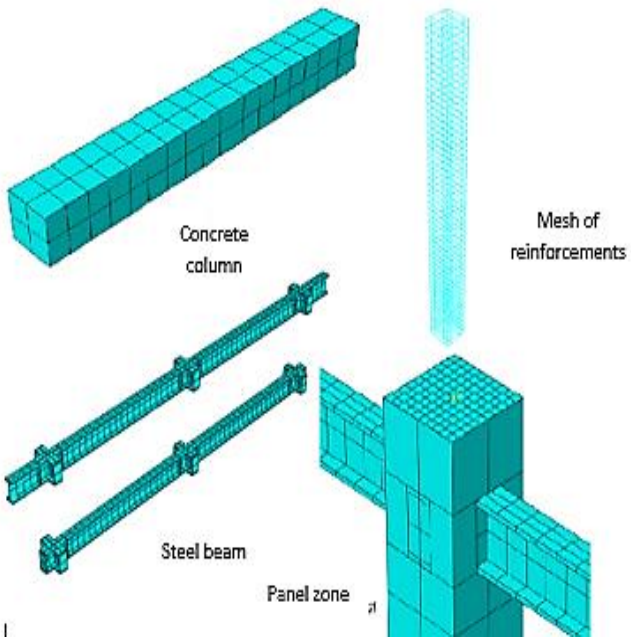

Fig. 4. The main members of the composite model (RCS) in ABAQUS.

In order to circumvent this situation, the concrete damaged plasticity model implemented in ABAQUS 2013 [20] was used herein. By experimental observations on most of quasi-brittle materials, including; concrete, when the load changed from the tension to compression, compression stiffness recovered with the closure of crack. Moreover, when the load changed from compression to tension, once the crushed micro-cracks occurred, and the stiffness in tension would not be restored. This performance corresponded to the default value w_t=0 and w_c=1 in ABAQUS. w_t and w_c were equal to the stiffness recovery factors. Figure 5 describes the default properties under uniaxial cyclic loading [21].

The CDP (Concrete damaged plasticity) model applied in the ABAQUS software was a modification of the Drucker–Prager strength hypothesis [21]. The ABAQUS user's manual specified default σ_{b0}/σ_{c0} = 1.16. It is worth mentioning that σ_{b0}/σ_{c0} was a ratio of the strength in the biaxial state to the strength in the uniaxial state (Fig. 6).

In this paper, in order to simplify the problem in the analysis of the finite element method, assuming that the ties and longitudinal reinforcement in concrete columns were ideal elasto-plastic materials, regardless of the reinforcement service stage and Bauschinger effected in their stress–strain relations. The stress–strain curve was sloped before the steel yields, and it would be simplified to horizontal line after that, as depicted in Fig. 7. The VonMises yield criterion with isotropic hardening model was adopted for structural steel.

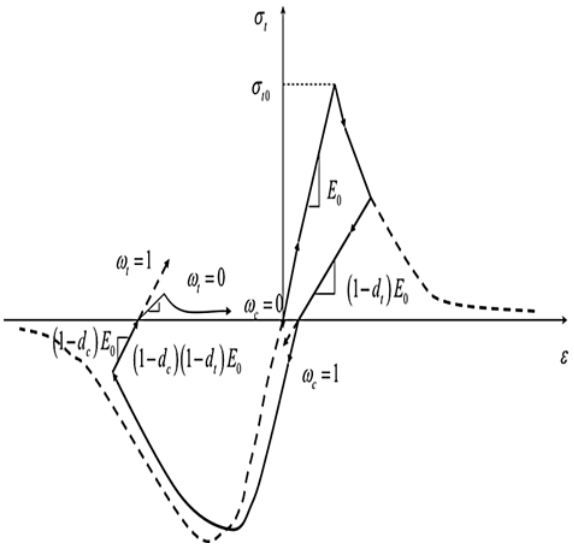

Fig. 5. Uniaxial load cycle (tension–compression–tension) assuming default values for the stiffness recovery factors: w_t=0and w_c=1 [21]

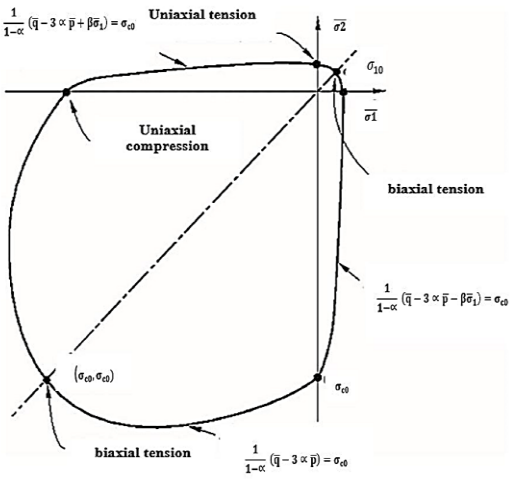

Fig. 6. Strength of concrete under biaxial stress in the CDP model [21]

The last parameter characterizing the performance of concrete under compound stress was dilation angle, i.e., the angle of inclination of the failure surface towards the hydrostatic axis, measured in the meridional plane. Physically, dilation angle ψ was interpreted as a concrete internal friction angle. In simulations, ψ was usually assumed to be 36° or 40°.

4. Determination of Constraints, Boundary Conditions and Loading

The boundary conditions and loading manners of RCS frame structures were specific in this paper: concrete column foot was fixed constraint, the axial load was applied by the loading plate on top of the column, and lateral load was used on the beam. In the ABAQUS software, the boundary conditions were set as follows: 3 concrete columns with fixed boundary constraints, the steel beam, and face bearing plates used the "Merge" command of the "Assembly" module to merge. In this case, steel beams and face bearing plates could be regarded as fixed constraints.

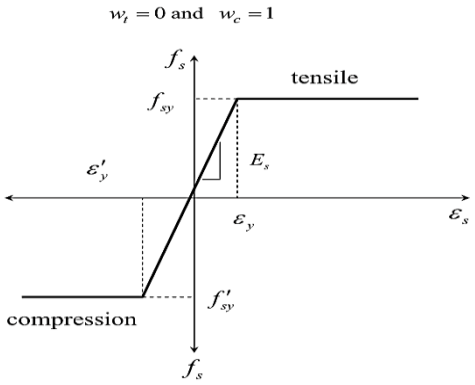

Fig. 7. Stress–strain relationship of reinforcement and structural steel [21].

The loading plate and the interface of column cap were constrained by the "Interaction" module "Tie" command. As illustrated in Fig. 8, The loading of the frame divided into two categories; the axial load at the top of the framed column and the lateral load at the end of framed beam. 2 load steps were required in the ABAQUS code in the load step as follows: at the top of 3 framed columns respectively applied to the axial load. Firstly, applied to interior column, and consequently to 2 other exterior columns.

When axial loading was completed, the lateral load would be loaded at both ends of the framed beam, and displacement loading adopted in order to acquire the load–displacement curves of the frame, that was, displacement applied at the end of the beam (applied displacement boundary conditions that known). In order to avoid stress concentration, the "Load" module "Pressure" of ABAQUS was adopted for the axial load and the analysis would not stop until the selected displacement was reached. Figure 8 shows the boundary conditions and loading pattern for the 2-story composite frame (RCS) in ABAQUS.

The axial load for the exterior column was 484.2 kN. The method of applying the cyclic loading on the frames was in accordance with the proposed method in ATC 24 [22]. Pursuant to this method, yielding displacement of models was the basis of applying cyclic loading.

The history of the cyclic loading was included in the range of incremental displacement in accordance with Fig. 9, in which δ was equivalent to the maximum displacement in the loading no. i. n_i was equivalent to the number of applied cycles with the range of displacement δ and Δ was equivalent to the yielding displacement (Δ=Δy). The material used in modelling of frame was given in Table 1.

There were several parameters in the software for the RC model, which could vary in a certain range pursuant to the type of model. Their appropriate values were determined by doing trial-and-error numerical method and comparing the output of the software with experimental results. For example, the method of meshing the geometric model, determining the appropriate values of parameters of damage of materials, and the viscosity coefficient could be pointed out. In this research, analytical results were compared with the experimental results of the specimens.

In order to adapt the responses, various parameters of modelling had been modified in some ways to achieve a favorable condition. After modeling the 3rd-frame in software, the components were connected to each other in the Assembly module, and were constrained in the Interaction module, then meshing parameters were defined in the Mesh module.

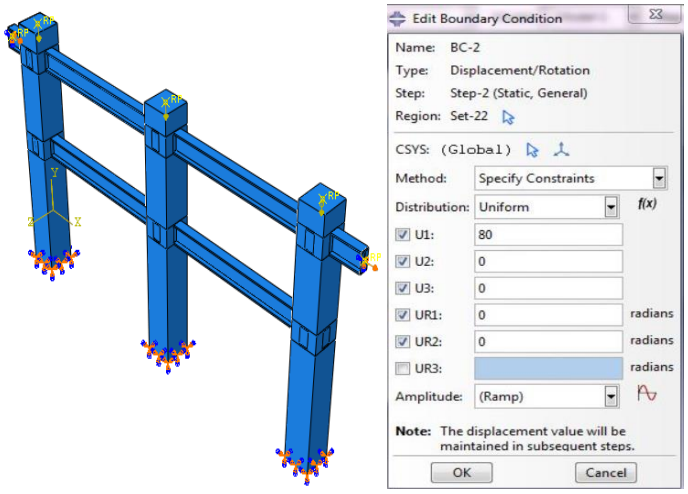

Fig. 8. Boundary conditions and Loading pattern for the Two-story Composite Frame (RCS) in ABAQUS

Table 1. Dimensions and material of elements of composite frame

Sections	Dimensions (mm)	Material	Compressive strength (N/mm²)	Tensile strength (N/mm²)	Elasticity modulus (10^4 N/mm²)
Column	300x300	Concrete	26.9	1.91	2.21
Beam	BH-200x100x12x16	Steel	312.4	463.9	19.7
Longitudinal reinforcement	12-D19 (ρ_t =1.28%)	Steel	385.4	556	17.7
Transverse reinforcement	4D-10 @ 50 (ρ_w =1.9%)	Steel	375.3	516.3	16.9

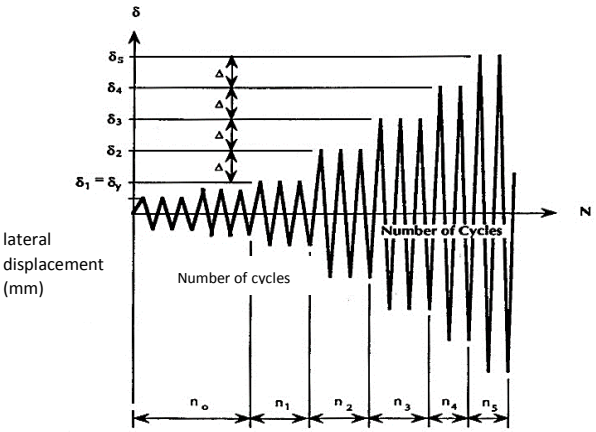

Fig. 9. The lateral displacement pattern based on ATC24 [22].

Applying the sensitivity analysis, it can be estimated the dimensions of meshing. In this analysis, the initial size of meshing in the beam was 8 cm, and the size of meshing in column elements was kept constant. Consequently, the model was subjected to static analysis and the force-displacement diagram was derived for analysis. After that, the size of the meshing was reduced, and analysis was performed again. This had done several times until obtained graphs had a minimal difference with each other. At last, by operating sensitivity analysis, the meshing dimensions of the beam element were selected to be 6 cm. Figure 10 shows variations of force-displacement for different sizes of meshing of elements.

5. Determining the Type of Analysis

The ABAQUS software has the capability of performing linear and nonlinear static and dynamic analysis. For verification of the model, a nonlinear pushover analysis had been used in order to consider the long-term effects of applied loads. As a result, static analysis was applied. The nonlinearity of an analysis depended on three factors: 1. Non-linearity of materials. 2. Non-linearity of geometry 3. Non-linearity of boundary conditions [20].

Non-linearity of boundary conditions occurred when boundary conditions changed during analysis. On that account, the model of this research was considered to have constant boundary conditions. The reasons for applying the non-linearity of the analysis were the non-linearity of materials and the non-linearity of the geometry of the model. Since the large deformation occurred during the analysis, this feature was provided with activating the Nlgoem option in the software [10].

6. The Results of the Analysis of the 2-Story Composite Frame (RCS)

After the composite frame (RCS) had been modeled in the software, the nonlinear static analysis was carried out by applying an incremental displacement to the end of the beam in the upper story, and results were depicted in Fig. 11 to 13.

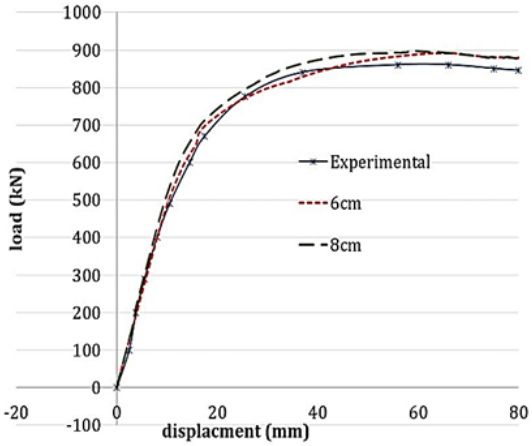

Fig. 10. variations of force- displacement for different sizes of meshing of elements

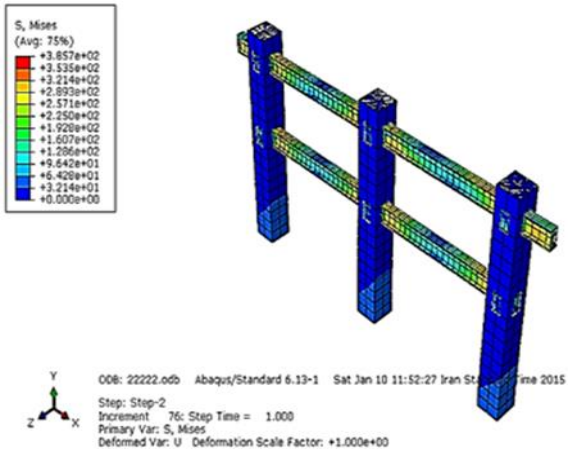

Fig.11. The Stress of 2- story composite frame (RCS) (N/mm²)

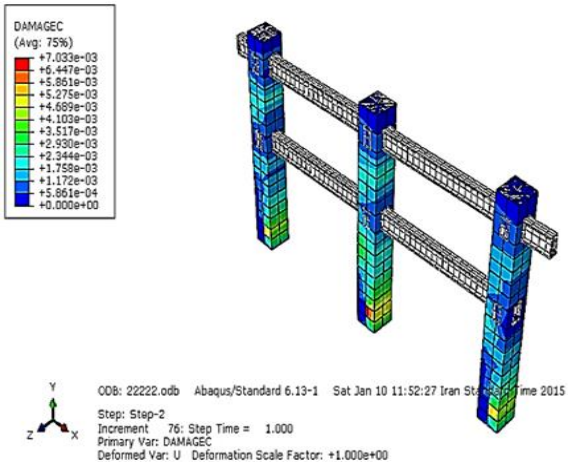

Fig.12. The compressive damage of concrete in 2- story composite frame (RCS)

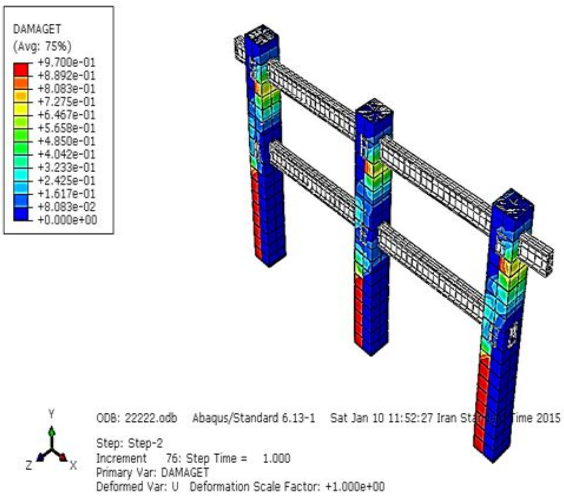

Fig.13. The tensile damage of concrete in the 2-story composite frame (RCS)

7. Introduction of Analytical Nonlinear Models

After verifying the selected experimental model, braces were added to the frame. Consequently, the effects of them on the frame behavior were inspected. In this model, 3 types of bracing were added, as presented in Table 2, including; X-braces (X), mega braces with 2 stories (2X), and chevron braces.

Pushover and cyclic analysis were performed on specimens, and the pushover analysis continued until the plastic hinge appeared in the column.

In the following, the load - displacement diagram of the analytical structure was compared with the experimental hysteresis cyclic pushover curve and, as illustrated in Fig. 14, it was in decent agreement with the experimental results. In Fig. 15, The diagram of cyclic load-displacement of the 2-story composite frame (RCS) is shown and its results are compared with experimental results.

8. Connection of Steel Bracing and the Composite Frame (RCS)

The connections were defined by the through beam, in order to connect the steel bracing to the composite frame (RCS). Hence, the plate, which was connecting braces to the frame, was welded to the steel beam and extended like a steel beam inside the column, then was buried in concrete (Fig. 16). The braces were welded to plates by hinged connection. The dimensions of the plates were 570×180×8 mm.

9. Failure Pattern of the Composite Frame (RCS)

In a composite frame (RCS) under axial load and horizontal load, when the horizontal load increased, moments at the end of the beam and column enhanced by the same proportion. When the moment of the beam and the column reached the ultimate flexural capacity, the plastic hinge was formed in that position.

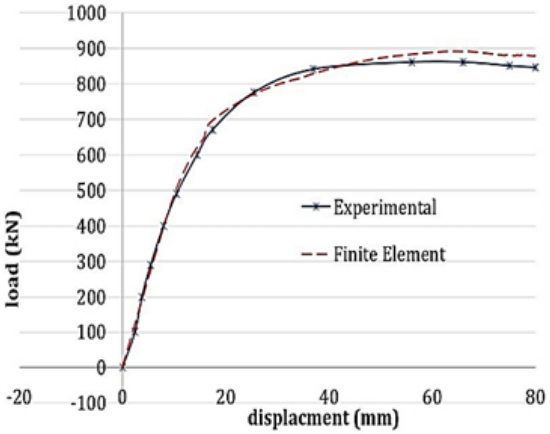

Fig.14. The load - displacement diagram of the 2-story composite frame (RCS)

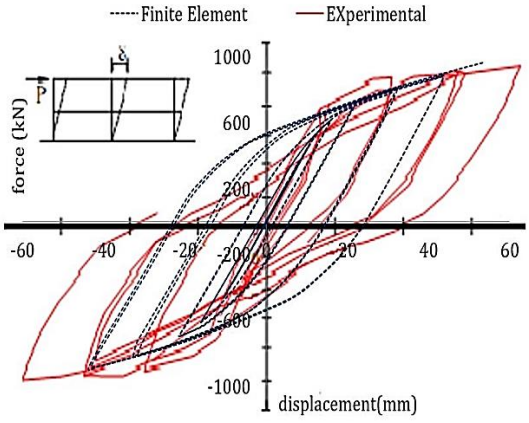

Fig. 15. The diagram of cyclic load - displacement of the 2-story composite frame (RCS) and its comparison with experimental results

Table 2. Composite Frame Models (RCS)

NO.	Type of structure	Seismic resistant system	Name of structure	Number of stories	Number of spans
1	RCS	RCS	Moment frame	2	1
2		RCS-brx	X-braces	2	1
3		RCS-br2x	Mega braces with two stories	2	1
4		RCS-brChevron	Chevron braces	2	1

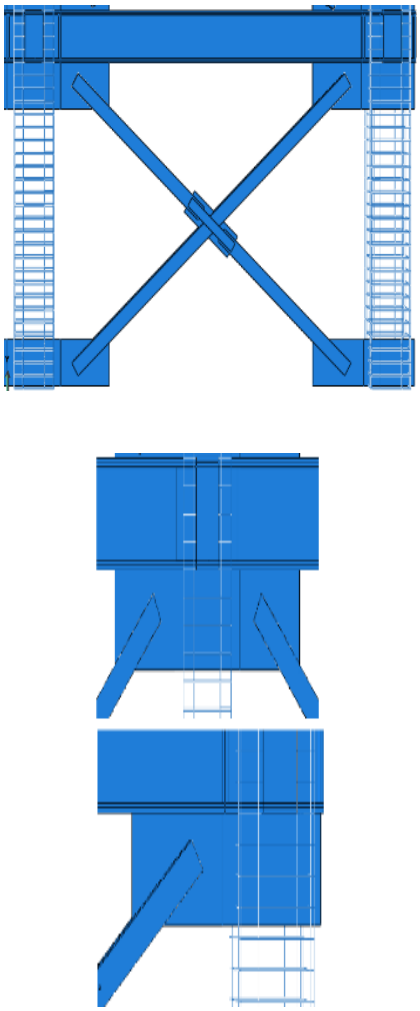

Fig.16. Connection of braces to the composite frame (RCS)

In order to design the composite frame (RCS), the requirements for "strong column - weak beam" and "strong connection - weak components" had to be considered. The yielding mechanism in the composite frame (RCS) would be such that plastic hinges were firstly formed at the end of the beam.

The formation of plastic hinges inside the columns would be strictly avoided. The development of a plastic hinge in the columns caused a lot of structural problems, including; decreasing the energy absorption capacity and structural ductility, creating a soft story, and large drift in the story in the columns, which were consisted of a large number of plastic hinges. In addition, rupture led to total failure in the structure. Fig. 17 reveals the yielding and failure stages of the composite frame model (RCS).

The first plastic hinge was formed by the flexural yielding in the flange of beam and the column in the first-story. The plastic hinges in the flange of the beams were appeared based on the number indicated in the Fig. 17. After the formation of the plastic hinge in the beam of the second-story (shown with the number 5), the first shear yielding appeared on the web of the beam at the place of the first plastic joint. Consequently, in the rest of plastic hinges, the web of the beam reached to shear yielding as well. Moreover, in the longitudinal reinforcements, the columns were subjected to the tensile and compressive yielding, and the plastic hinges were firstly formed in the middle column and then in the lateral columns. These results were compared with the results acquired from the experiment.

Experimental results showed that the first plastic hinges occurred at the base of columns, and the reasons for these difference results could be explained by the effect of the axial load above the column. In the experiment, the axial load above the column was changed by increasing the horizontal load, but the axial load was constant in the analysis. With increasing horizontal load, the column had deformation, while the axial force at the top of the column decreased. To compensate for the lost axial load, the axial load on the column was applied incrementally.

As a result, a synthetic increase happened in the axial load above the column, which led to increasing the moment at the base of the column. On that account, longitudinal reinforcement at the base of the column yielded much earlier. Generally, in analytical and experimental results, plastic hinges were firstly appeared at the end of the beam near to the panel zone and then in the longitudinal reinforcements at the base of columns.

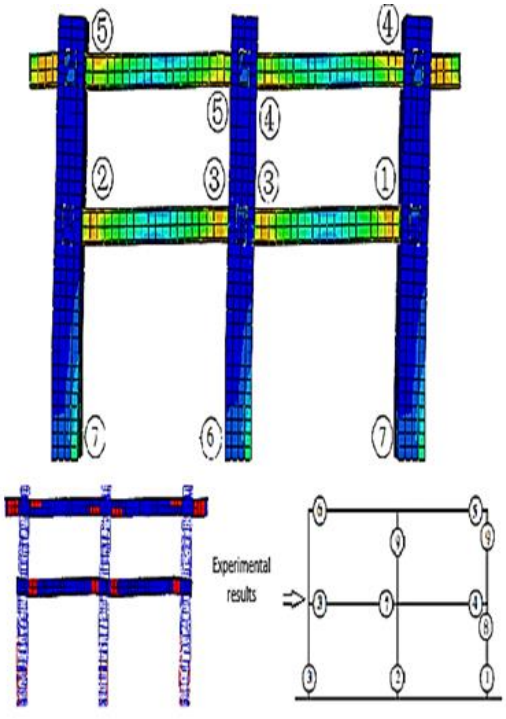

Fig.17. The arrangement of formation of plastic hinges in the composite frame (RCS)

10.Investigating the Results of Braced RCS Frame Analysis

In order to explore the nonlinear behavior of braced composite frame (RCS), three types of braces were added to the verified model, including; x braces, mega braces with 2 stories, and chevron braces. In Figs. 18 to 20, the stress acquired from the analysis of these models is illustrated. Figure 21, diagrams of load - displacement of these structures were compared.

The ultimate strength in the RCS composite frame with one - third scale without bracing was 890.77 kN. On the other hand, maximum force of RCS-brx was 1.77 times more, and the maximum force of RCS-br2x was 1,2 times more, and the maximum force of RCS-brChevron was 1.37 times more than RCS frame. The braces enhanced the yielding resistance and stiffness of the frame, as well.

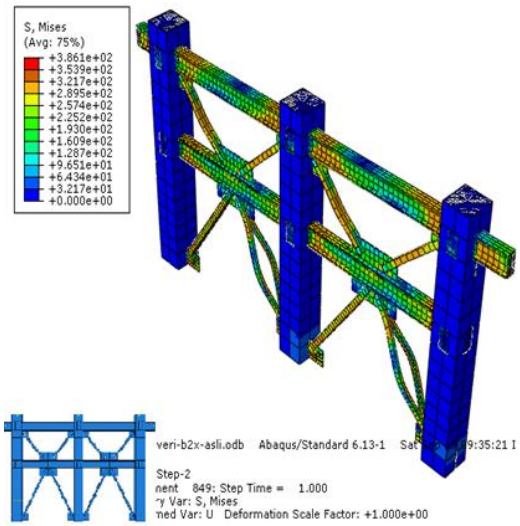

Fig.18. The stress in RCS frame with mega braces (RCS-br2x) (N/mm²)

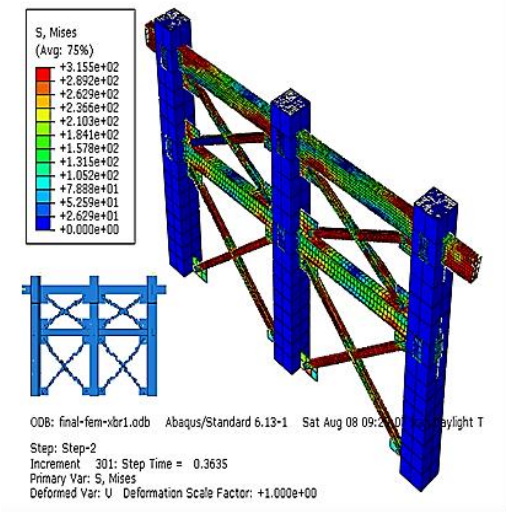

Fig.19. The stress of 2- story RCS frame with X-bracing (RCS-brx) (N/mm²)

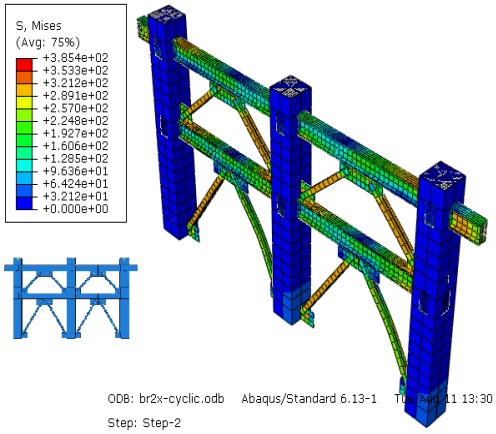

Fig.20. The stress of 2- story RCS frame with chevron bracing (RCS-brChevron) (N/mm²)

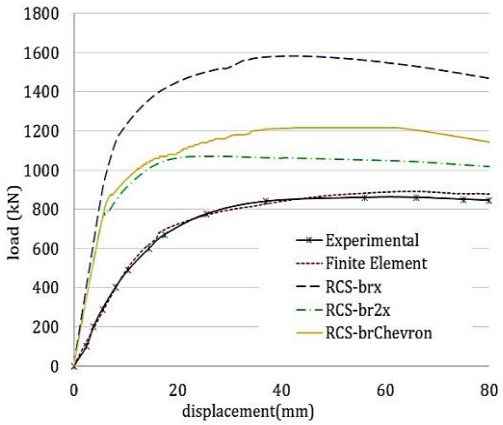

Fig.21. Diagram of load- displacement of the composite frame (RCS) with bracing

11. Investigation of Primitive-Stiffness of Models

the stiffness or rigidity of a structure was defined as the amount of required force in order to create a unite displacement [23]. Therefore, to determine the stiffness, the location and the type of expected displacement had to be specified accurately. Stiffness was one of the determinant factors in resistant systems against earthquakes, such as bracing systems and shear walls, which were determined by the diagram of load – lateral displacement. In Fig. 22. an example of these graphs was depicted in a schematic diagram.

In the mentioned diagram, the slope of the line OA was defined as the structural stiffness, and F_u was defined as ultimate strength. As shown in Fig. 17, the relationship between load and lateral displacement in the elastic zone was based on Eq. (1).

$$F = KU \tag{1}$$

In order to compute the stiffness of the structure at any desired level, the Eq. (2) can be contemplated.

$$K = F/U \tag{2}$$

In Table 3, the primitive stiffness of the composite frames was calculated pursuant to Fig. 23. The braces increased the average stiffness of the RCS frame about 3 times; primitive stiffness of X braces (RCS-brx) was more than other braces (RCS-brChevron and RCS-br2x).

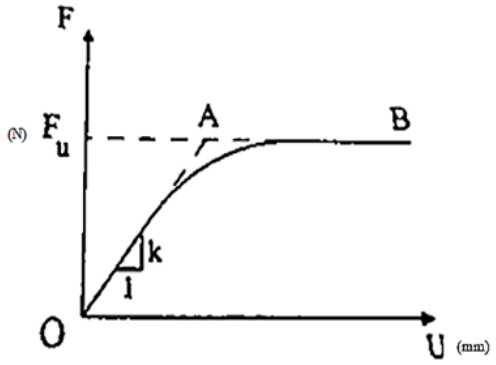

Fig. 22. Displaying the primitive-stiffness in the diagram of load- displacement [23]

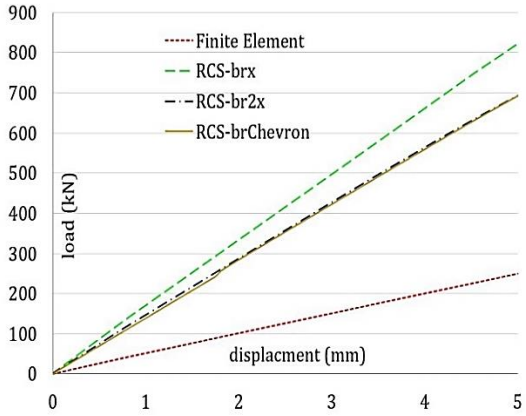

Fig. 23. Primitive stiffness in the diagram of load-displacement of composite frames

Table3. The early hardness of composite frames

Name	F (kN)	U (mm)	K	Amount of increase of primitive stiffness relative to the RCS frame
RCS	250	5	50	-
RCS-brx	815	5	163	3.26
RCS-br2x	690	5	138	2.76
RCS-brChevron	690	5	138	2.76

As a result of the necessity of controlling the displacement of structures, the stiffness of the resistant systems against earthquake was very important. Naturally, as it was discovered in Table 3, systems, that had more stiffness, had less lateral displacement against their lateral loads.

12.Behavior factor

The behavior factor was a factor that converted elastic force into a design force based on seismic codes. The amount of the behavior factor depended on the amount of structural ductility.

Designing structures for elastic behavior under the vibrations caused by large earthquakes was not economical, and therefore most buildings were designed for shear force. The shear force was far less than the yielding force of the strongest earthquake that was likely to occur. Structures had a non-elastic behavior during the earthquake and dissipated a large amount of induced seismic energy by the plastic deformation in the form of the residual energy. Computing the amount of dissipated energy, due to inelastic performance and accurate, designing and analyzing pursuant to the actual behavior of the structure required to perform non-linear analysis. Therefore, its complexity and its consuming time led to the above analysis was not applied in practice. In seismic design codes, reduced forces due to various phenomena of damping, ductility, and etc., were calculated from the division of the earthquake linear spectrum into behavior factor.

13. The Method of Determining the Behavior Factor

The behavior factor could be computed pursuant to the Uang [24] method. According to this method, the behavior factor was acquired based on equation (3):

$$R = R_\mu R_s \gamma \tag{3}$$

In which R was the behavior factor, R_μ was the ductility factor, R_s was the over strength factor, and γ was the allowable stress factor. The over strength factor connected the design force to the equivalent yielding force of the structure. On that account, R was mostly greater than one. As a result, structures were designed for less force than the force that made complete plastic behavior. In order to compute the behavior factor of frames, Uang had carried out extensive research. In Fig. 24, the actual response of the load - displacement and the linear assumptive response of a structure were illustrated.

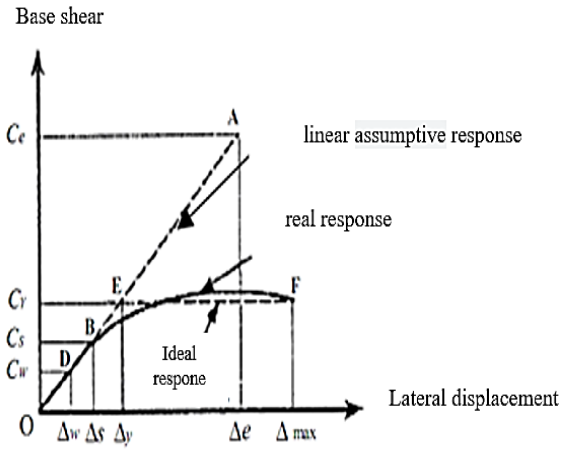

Fig.24. The overall response curve of structures in the elastic and inelastic modes

The linear force reduction was expressed in terms of yielding force (Cy) by the force reduction factor as a result of its ductility (Rμ).

$$R_{\mu} = \frac{C_e}{C_y} \quad (4)$$

This factor represented the energy dissipating capacity in the plastic behavior of the structure and was related to the coefficient μ. Various relationships had been proposed to determine Rμ like relationship proposed by Newmark and Hall [24] in 1982. By applying it, it could reduce the ductility factor (Rμ) for a complete plastic-elastic system with a single-degree of freedom as follows:

For a period-time less than 0.03 seconds (frequencies more than 33 Hz):

$$R_{\mu} = 1 \quad (5)$$

For the period time between 0.12 Second and 0.5 Second (frequencies between 2 and 8 Hz):

$$R_{\mu} = \sqrt{2\mu - 1} \quad (6)$$

For period time more than 0.1 seconds (frequencies are less than 1 Hz):

$$R_{\mu} = \mu \quad (7)$$

μ ≤1 represented elastic behavior, and μ> 1 indicated inelastic behavior, and μ was the degree of ductility.

In order to convert the behavior factor to the behavior factor of the Iranian earthquake codes and standard No. 2800-05, the amount of allowable stress factor could be considered between 1.33 and 1.44. In this study, the factor was equal to 1.4. As observed above, the calculation of the amount of Rμ depended on the determination of the amount of period time of every structure. For this purpose, a modal analysis was achieved for each of the structures, and its values were presented in Table 4.

Table 4. Period time of composite frame models (RCS)

Name of the model	Period time	Percent of reduction in the period time relative to the moment frame RCS
RCS	0.8565	–
RCS-brx	0.4556	46.80
RCS-br2x	0.4975	41.92
RCS-brxChevron	0.4974	41.92

As depicted in Table 4, the period times of the bracing systems were between 0.12 and 0.5, and as a result, the coefficient of reduction (due to the ductility) of these structures were acquired from equation (6). Moreover, the period time of the composite moment frames (RCS) was between 0.12 and 0.5, and the reduction coefficient of the ductility in this structure was obtained by interpolation of values obtained from equations (6) and (7). Despite that, in actual structures, the number of stories and spans could have an effect on the study of the period time, but in this study, frames were deliberated to gain a limited number of stories and spans.

14. Investigation of Ductility and Behavior Factor in Composite Frames (RCS)

Increasing the ductility resulted in increasing energy absorption under lateral and earthquake loads. Structures were divided into three groups with high ductility, average ductility, and ordinary ductility in terms of ductility. This classification was mostly based on the maximum displacement ratio to the yielding equivalent displacement. The more this ratio was, the more the ductility was. Applying the MATLAB software [25] and FEMA code [26], an ideal bilinear curve was drawn.

In Fig. 25, Yy and Yu, respectively, were yielding and ultimate displacement, FY and Fu were the yielding and the ultimate strength of the analytic models, and the ideal bilinear behavior was drawn in such a way that the two areas of A1 and A2 became equal.

Pursuant to the results of finite element analysis, in Table 5, the amount of ductility and behavior of these structures was indicated.

15.Conclusions

- It had been widely recognized from previous research, that composite moment frames consisting of RC columns and steel (S) beams, or the so-called RCS system could provide a cost-effective alternative to traditional

steel or RC construction in seismic regions. On that account, problems associated with connections were significantly reduced, and the RCS frames were generally more economical than the pure steel or RC moment frames.

- Applying braces and increasing the number of spans made the composite frame (RCS) more ductile and increased behaviour factor.
- By comparing the behaviour of the braced RCS frame, it could be seen that RCS-br2x had better behaviour and, it increased the stiffness of the structure, as well as increased the ductility more than other studied braces.
- The behaviour factor of the examined structures could be 5.7 averagely.
- It will be suggested that the behaviour of these structures would analyse by using other types of seismic systems, including; steel shear walls, concrete shear walls, and so on in terms of performance and implementation.
- Generally, the reinforcement of the RCS frame by bracing had positive effects on the hardness and ductility. It also showed that the presence of bracing in the RCS frame delayed the start of cracking and reduced lateral displacement under the lateral load.

References

[1] Griffis, L.G., (1986). Some design considerations for composite-frame structures. *Engineering Journal, AISC*. p. 59-64.

[2] Sheikh, T.M., Deierlein, G.G., Yura, J.A. and Jirsa, J.O., (1989). Beam-column moment connections for composite frames: Part 1. *Journal of Structural Engineering*. 115(11): p. 2858-2876.

[3] Kheyroddin, A., Naderpour, H. and Ahmadi, M., (2010). Reviewing the Behavior and Comparison of the World's Most Reliable Codes in the Field of Concrete and Steel Compound Columns. *Journal of Modeling in Engineering*. p. (Eighth): p. No. 22.

[4] Deierlein, G., Design of Moment Connections for Composite Frames. 1988, Ph. D. Dissertation, University of.

[5] Becheri, T., Amara, K., Bouazza, M., & Benseddiq, N., (2016). Buckling of symmetrically laminated plates using nth-order shear deformation theory with curvature effects. *Steel and Composite Structures*. 21(6): p. 1347-1368.

[6] Bouazza, M., Lairedj, A., Benseddiq, N. and Khalki, S., (2016). A refined hyperbolic shear deformation theory for thermal buckling analysis of cross-ply laminated plates. *Mechanics Research Communications*. 73: p. 117-126, doi: https://doi.org/10.1016/j.mechrescom.2016.02.015.

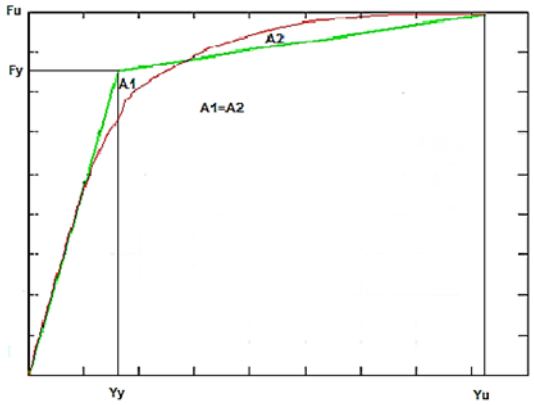

Fig.25. Required parameters for calculating behavior factors in load - displacement diagrams [26].

Table 5. Calculating the behavior factor of the composite models RCS

Name of models		RCS	RCS-brx	RCS-br2x	RCS-brChevron
Ultimate load	Fu(kN)	879.17	1466.5	1043.12	1251.706
Ultimate displacement	Yu(mm)	77	79.786	65.275	60.578
Yielding load	Fy(kN)	800	1482.48	1015	1060
Yielding displacement	Yy(mm)	17	9.092	7.9	7.5
Ductility	μ=Yu/Yy	4.53	8.8	8.26	8.08
Percent of increase of ductility of models in comparison with moment frame (%)	-	-	73.73	94.26	82.34
Ductility factor	Rμ	3.7	4.074	3.94	3.89
Over strength factor	Rs=Fu/Fy	1.1	0.99	1.03	1.18
Proposed allowable stress factor	γ	1.4	1.4	1.4	1.4
Behavior factor	R	5.69	5.64	5.67	6.43

[7] Bouazza, M., Kenouza, Y., Benseddiq, N. and Zenkour, A.M., (2017). A two-variable simplified nth-higher-order theory for free vibration behavior of laminated plates. *Composite Structures*. 182: p. 533-541, doi: https://doi.org/10.1016/j.compstruct.2017.09.041.

[8] Antar, K., Amara, K., Benyoucef, S., Bouazza, M., & Ellali, M., (2019). Hygrothermal effects on the behavior of reinforced-concrete beams strengthened by bonded composite laminate plates. *structural engineering and mechanics*. 69(3): p. 327-334.

[9] Bouazza, M., Benseddiq, N. and Zenkour, A.M., (2019). Thermal buckling analysis of laminated composite beams using hyperbolic refined shear deformation theory. *Journal of Thermal Stresses*. 42(3): p. 332-340, doi: 10.1080/01495739.2018.1461042.

[10] Hemmati, A., & Kheyroddin, A., (2011). Investigation of transition story effect on behavior of vertically hybrid buildings.

[11] Bakhshayesh Eghbali, N. and Mirghaderi, S.R., (2017). Experimental investigation of steel beam to RC column connection via a through-plate. *Journal of Constructional Steel Research*. 133: p. 125-140, doi: https://doi.org/10.1016/j.jcsr.2017.02.007.

[12] Cheng, C.-T. and Chen, C.-C., (2005). Seismic behavior of steel beam and reinforced concrete column connections. *Journal of Constructional Steel Research*. 61(5): p. 587-606, doi: https://doi.org/10.1016/j.jcsr.2004.09.003.

[13] Bazzaz, M., Andalib, Z., Kafi, M. A., & Kheyroddin, A., (2015). Evaluating the performance of OBS-CO in steel frames under monotonic load. *Journal of Earthquakes and Structures*. 8(3): p. 697-710.

[14] Ghods, S., Kheyroddin, A., Nazeryan, M., Mirtaheri, S.M. and Gholhaki, M., (2016). Nonlinear behavior of connections in RCS frames with bracing and steel plate shear wall. *Steel and Composite Structures*. 22(4): p. 915-935.

[15] Le, D., Nguyen, X. and Nguyen, Q. (2017). Numerical Study on a New Through-Column-Type Joint for RCS Frame. in *International Conference on Advances in Computational Mechanics*. Springer.

[16] Mirghaderi, S.R., Eghbali, N.B. and Ahmadi, M.M., (2016). Moment-connection between continuous steel beams and reinforced concrete column under cyclic loading. *Journal of constructional steel research*. 118: p. 105-119.

[17] Kheyroddin, A. and Madah, Z., (2018). Analyzing the Behavior of Hybrid Steel System of Tube in Tube with Bracing and Belt Truss. *Numerical Methods in Civil Engineering*. Vol. 2, No. 3.

[18] Iizuka, S., Kasamatsu, T. and Noguchi, H., (1997). Study on the aseismic performances of mixed frame structures. *J Struct Constr Eng Archit Inst Japan*. 497: p. 189-96.

[19] Li, W., Li, Q.-n., Jiang, W.-s. and Jiang, L., (2011). Seismic performance of composite reinforced concrete and steel moment frame structures–state-of-the-art. *Composites Part B: Engineering*. 42(2): p. 190-206.

[20] (2013). ABAQUS 6.13 Analysis User's Manual. volume III.

[21] Kmiecik, P. and Kamiński, M., (2011). Modelling of reinforced concrete structures and composite structures with concrete strength degradation taken into consideration. *Archives of civil and mechanical engineering*. 11(3): p. 623-636.

[22] Council, A., (1992). Guidelines for cyclic seismic testing of component of steel structures. *Redwood City, CA: ATC-24*.

[23] Wenham, M., Stiffness and Flexibility. 200 science investigations for young students. 2005, ISBN 978-0-7619-6349-3.

[24] Wilson, R.R., Rojahn, C. and Sharpe, R.L. (1985). Earthquake damage evaluation data for California. ATC.

[25] www.mathworks.com.

[26] FEMA p695 Quantification of building Seismic Performance factors.